GSC

GENERAL SOFTWARE CORPORATION

SPACECRAFT ATTITUDE CALIBRATION/VERIFICATION BASELINE STUDY

Prepared for
GODDARD SPACE FLIGHT CENTER

By
Dr. Lily C. Chen
GENERAL SOFTWARE CORPORATION

Under
Contract No. NAS5-26205
February 28, 1981

ABSTRACT

This document presents a baseline study for a generalized spacecraft attitude calibration/verification system. It can be used to define software specifications for three major functions required by a mission: the pre-launch parameter observability and data collection strategy study; the in-flight sensor calibration; and the post-calibration attitude accuracy verification. Analytical considerations are given for both single-axis and three-axis spacecrafts. The three-axis attitudes considered include the inertial-pointing attitudes, the reference-pointing attitudes, and attitudes undergoing specific maneuvers. The attitude sensors and hardware considered include the Earth horizon sensors, the plane-field Sun sensors, the coarse and fine two-axis digital Sun sensors, the three-axis magnetometers, the fixed-head star trackers, and the inertial reference gyros. A review of the calibration/verification procedure currently performed on the Solar Maximum Mission (SMM) is also presented.

TABLE OF CONTENTS

TABLE OF CONTENTS (Cont'd)

LIST OF ILLUSTRATIONS

Figure

LIST OF TABLES

Table

SECTION 1 - INTRODUCTION

1.1 BACKGROUND AND MOTIVATIONS

The spacecraft sensor calibration/verifcation support for attitude determination and control will become the primary ground support activity during the coming decade. The calibration support includes the determination of the sensor characteristics and alignments from which the sensors can be correctly modeled and the attitude can be accurately computed from the sensor measurements. The verification support consists of the comparison between the attitude computed on-board with that computed on the ground and the indication of requirements for new calibration updates. In the past, this calibration/verification function was performed by tailor made software systems implemented to meet the mission requirements for specific missions. Due to the similarities in missions and sensors, many of these efforts were redundantly performed. Thus, the cost of such activity can be largely reduced if a baseline is available from which the mission software specifications can be defined for all mission requiring calibration/verification support.

The purpose of this baseline study can be summarized as follows:

* To generalize the in-flight calibration/verification procedures to reduce redundant efforts for missions carrying similar sensors.
* To help in developing general-purposed softwares to perform pre-launch attitude and bias observability studies so that
  (1) data acquisition schemes to optimize bias observabilities can be planned prior to

the mission and schedules into the mission time line.

(2) Sensor configuration and orientations can be planned prior to the mission to optimize the attitude and bias determination geometries.

(3) Unnecessary efforts attempting to improve the attitude accuracy to below the geometrical limit can be eliminated.

(4) Unnecessary efforts attempting to determine more than enough biases can be reduced.

(5) Unnecessary efforts attempting to determine biases from inadequate or improper data sets can be reduced.

(6) Reliable estimates for attitude determination accuracies can be obtained.

* To simplify the calibration/verification software developments and operations by unifying the basic calibration algorithms and by sharing as many of the software modules as possible among sensors and missions.

1.2 DOCUMENT OVERVIEW

To achieve the above goals, a review of calibration/verification procedure currently being performed on the Solar Maximum Mission (SMM) is given in Section 2 to study its accuracy, possible enhancements, and feasibility on other missions. Based on the SMM procedure, a generalized baseline is then developed from which future calibration and verification functions can be fashioned. This baseline is presented in Section 3 of the document. From this baseline, software specifications for the following three major functions required by each mission

can be defined: (1) Pre-launch parameter observability and data collection strategy study; (2) In-flight sensor calibration; and (3) post-calibration verification. Finally, the analytical basis of the baseline and the equations required for each of the software modules included in the baseline are presented in Section 4. In these analytical considerations, both the inertial and the reference-pointing spacecrafts are included. The attitude sensors and hardwares considered include the Earth horizon sensors, the plane-field Sun sensors, the coarse and fine two-axis digital Sun sensors, the fixed-head Star trackers, the inertial reference gyros, and the three-axis magnetometers.

SECTION 2 - CURRENT SMM CALIBRATION/VERIFICATION PROCEDURE

The SMM is the first of the Multimission Modular Spacecraft (MMS) series. The scientific objective of the mission is the study of the complex solar flare phenomena. The spacecraft was launched into a near-circular orbit on February 14, 1980. The attitude determination and control hardware onboard the spacecraft includes two coarse Sun sensors (CSS), one fine Sun sensor (FSS), two fine pointing Sun sensors (FPSS), two fixed-head star trackers (FHST), two three-axis magnetometers (TAM), and one inertial reference unit (IRU) which contains three gyros, four reaction wheels, six magnetic torquing coils, and one onboard computer (OBC). To meet the attitude determination and control accuracy requirements, sensor calibration/verification activities were performed by the SMM Attitude Ground Support System Software (AGSSS). The AGSSS consists of six independent subsystems. Two of them are responsible for the calibration/verification functions: the SMM Attitude Determination Subsystem (SMM/ADS)[1,2] and the SMM Fine Pointing Sun Sensor Off-Null Calibration Subsystem (SMM/FOCS)[3]. The SMM/ADS was used to calibrate the three-axis magnetometers, the fixed-head star trackers, and the inertial reference gyros; and the SMM/FOCS was used to perform the FPSS off-null calibrations.

These sensor calibration activities[4] are reviewed in the following subsections. Four areas are addressed for each type of sensor: The bias parameters defined, the calibration method used, the calibration results obtained, and a discussion of results. Some general comments on each of the calibration procedures are also presented to

serve as a guideline for future sensor calibration considerations.

2.1 THREE-AXIS MAGNETOMETER

2.1.1 Calibration Procedures and Results

The TAM measures the geomagnetic field in the spacecraft body coordinate which is used in conjunction with one of the Sun sensor measurements to provide a coarse attitude determination by the Coarse Attitude Determination Subsystem (CADS) in SMM/ADS. The TAM measurements are also used for momentum unloading. Thus, reliable magnetometer calibration is essential for both coarse attitude determination and spacecraft momentum management.

The CADS is also responsible for the TAM calibration function. The calibration parameter defined in this function is a constant bias vector on the measured geomagnetic field. The CADS uses an iterative least-squares technique to minimize the differences between the magnitudes of measured geomagnetic field and that computed from a mathematical model. The following conclusions were obtained as a result of the SMM magnetometer calibration activities:

(1) The magnetometer bias determined from a short interval can be totally unreliable.

(2) The magnetometer bias can be accurately determined by processing either a full orbit of data or two 10 minute data passes separated by approximately 30 minutes.

(3) Properly determined magnetometer biases remain relatively stable over long time periods.

2.1.2 Discussions and Comments

Some general comments and discussions on the SMM magnetometer calibration procedures and results are given in

the following:

(1) In general, two types of systematic errors are likely to affect the TAM measurements: the sensor misalignments and uncompensated magnetic field contaminations. The former can cause an orientation error on the measured geomagnetic field while the latter causes a residual bias on the measurement. In the current SMM procedure, only the latter is modeled and determined. No attempt was made in calibrating the TAM sensor alignment parameters. This is reasonable so far as attitude determination at inertial attitude is concerned because the effect on data due to the sensor misalignment cannot be distinguished from that due to attitude errors. In other words, the sensor misalignment parameters can be determined only when the attitude is determined through other means. In this case, the accuracy of the sensor alignment is the same as that of the attitude, and the sensor misalignment parameters so determined can certainly not be used to further improve the attitude accuracy. However, a good TAM calibration can always improve the performance of the momentum unloading. Thus, it would be desirable to include the capability of determining the misalignment parameters in TAM calibration procedure so far as the momentum management is concerned. In this case, the TAM alignment can be determined when the attitude is accurately determined by FPSS and FHST. The calibrated TAM can then be used to assist the momentum unloading process.

In fact, the effects due to TAM misalignments and attitude errors are likely to be separated if proper slew maneuvers are performed. However, performing slew maneuvers during the early phase of the mission may not be

permissible operationwise.

(2) The constant magnetometer bias vector can be separated from the attitude error because the former changes the magnitude of the measured geomagnetic field while the latter does not. Therefore, it is a good choice to use the magnitude of the geomagnetic field as the observable in the least-square filter. This enables the determination of the magnetometer bias regardless of the accuracy of the attitude. However, as the spacecraft position changes along the orbit, the direction of the geomagnetic field $\underline{B}$ also changes. Depending on the instantaneous direction of the geomagnetic field, a constant bias can give very different effects on its magnitude. For instance, a bias in $\hat{z}$ direction gives maximum effect on the field magnitude, B, if $\underline{B}$ is along $\hat{z}$ direction; but gives essentially no effect on B if $\underline{B}$ is along $\hat{x}$ or $\hat{y}$ direction. Thus, very different results in the bias vector $\underline{b}$ can be obtained if short data passes are used. On the other hand, when data from a long period in orbit is used, the variation in B readily tells the direction and magnitude of the bias $\underline{b}$. The more variation of $\underline{B}$, the better for determining $\underline{b}$. This explains the first two conclusions resulting from the SMM magnetometer bias determination. In fact, $\underline{B}$ goes through approximately a cycle every half orbit period (about 48 minutes). Therefore, a data pass with data uniformly distributed over a half-orbit period should be ideal for determining the magnetometer bias.

Actually, the amount of variations in the geomagnetic field directions within a half-orbit period differs strongly depending on the relative directions among the Earth pole, $\hat{z}$, the orbit pole, $\hat{s}$, and the geomagnetic

dipole, $\hat{m}$. For a given set of orbit parameters, the directions of $\hat{z}$ and $\hat{s}$ are fixed in the inertial space while the vector $\hat{m}$ rotates about $\hat{z}$ once a day with an angular separation of about 11.4 degrees from $\hat{z}$. Figure 2.1 shows the approximate variation in $\hat{B}$ during a half-orbit period when a simple dipole model is assumed for the geomagnetic field. The two cases shown in Figure 2.1 correspond to the two extreme cases when $\hat{m}$ is coplaner with $\hat{s}$ and $\hat{z}$. As can be seen from the figure, the amount of variation in $\hat{B}$ reaches maximum when $\hat{m}$ is in the direction of $\hat{m}_2$ which is coplaner with $\hat{s}$ and $\hat{z}$ but away from $\hat{s}$. Thus, the data pass chosen for the TAM bias determination will be optimal if the orbit time is chosen to satisfy this geometrical condition.

2.2 FIXED-HEAD STAR TRACKER

2.2.1 Calibration Procedures and Results

The FHSTs measure the star directions in the spacecraft body coordinate. These measurements, together with the FPSS measurements, are used by the Fine Attitude Determination Subsystem (FADS) of SMM/ADS to provide fine attitude determinations. Since the FPSS measurements can only determine the pitch and yaw angles when the spacecraft roll axis is pointing within 0.5 degrees about the Sun, the FHST measurements are responsible for the roll angle determination for all attitudes as well as the fine attitude determinations when the spacecraft is slewed away from the Sun. Thus, reliable FHST calibrations are essential for accurate attitude determinations.

The FHST calibration function is also performed by FADS. Two types of parameters were calibrated for SMM: The scale factors used to transform the measurements from

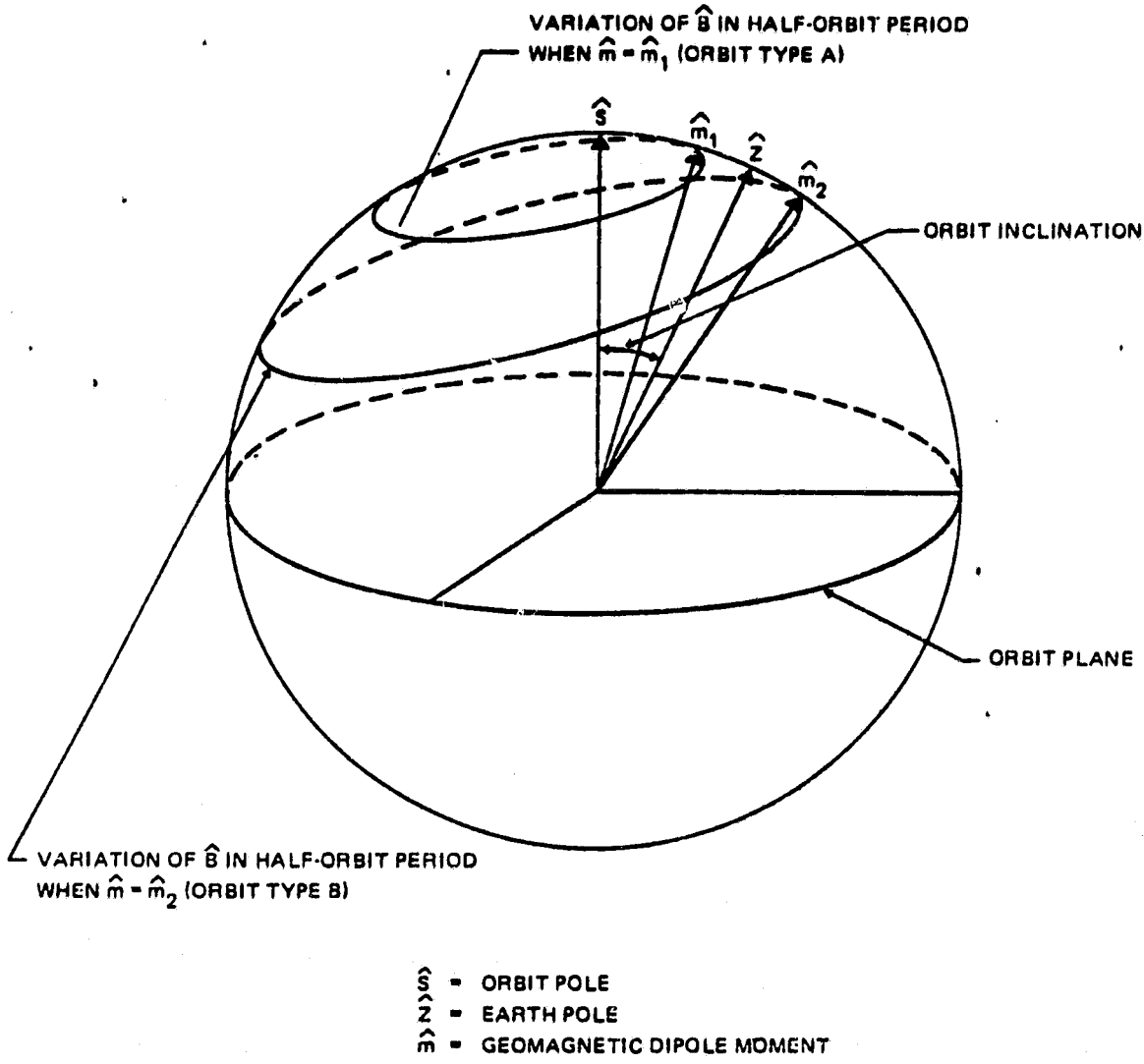

Figure 2-1. Variations in Geomagnetic Field Directions During Half-Orbit Period.

raw counts to angles, and the sensor misalignment parameters. The methods used to determine these parameters and the calibration results are described below.

2.2.1.1 Calibration Methods for Scale Factor Determination

Two methods were used in determining the FHST scale factors: the angular separation method and the empirical partial derivative method. In the angular separation method, the angular separations between stars observed by FHST were compared with that computed from the catalog stars. The scale factors, which were assumed to be constants, were then determined by minimizing the differences between observed and computed angular separations. In the empirical partial derivative method, the errors in scale factors were determined from the discrepancies between the attitudes determined from FHST and FPSS through partial derivative expressions. In these expressions, the scale factor errors were assumed to be the only error source that contributed to the attitude discrepancies.

2.2.1.2 Calibration Methods for Misalignment Determination

The FHST misalignment parameters were determined through an empirical partial derivative method similar to that used in the scale factor determination. In this method, the misalignment angles were computed from the discrepancies between the attitudes determined from FHST and FPSS through partial derivative expressions. Here, the FHST misalignment parameters were assumed to be the only error source that contributed to the attitude discrepancies.

2.2.1.3 Calibration Results

The following results were obtained from the SMM FHST calibration activities:

(1) The scale factor determination in general did not improve the FHST attitude determination accuracy regardless of the method used.

(2) The misalignment determination did improve the agreement between the attitudes determined from FHST and FPSS.

(3) Calibration in roll direction was not possible from the current method because the reference roll angle could not be obtained from FPSS.

(4) The uncertainty in α_1 determination (misalignment about $\hat{x}_{FHST}$, the FHST boresight) is much higher than the uncertainty in α_2 determination (misalignment about $\hat{z}_{FHST}$).

2.2.2 Discussions and Comments

In the following, some general comments and discussions on the SMM FHST calibration procedures are summarized.

(1) Among the two methods used in the scale factor determination, the angular separation method should be a better method to use because the angular separations between stars are independent of both the attitude and the sensor misalignments. Thus, using the angular separations between stars as observables, the scale factors can, in principle, be determined regardless of the attitude and sensor alignment accuracies.

(2) The attitude accuracy was not improved by the scale factor determination suggests that the scale factor error is probably insignificant comparing with other error sources.

(3) The FHST attitude and bias determination results obtained from single tracker may have high uncertainties due to geometrical limitations. The uncertainty is especially high for the orientation of the spacecraft about the FHST boresight, as demonstrated by the high uncertainty in the α_1 determination. This situation is analogous to that of FPSS where the orientation of the spacecraft about the FPSS borsight (the roll angle) is totally undeterimined. However, if both star cameras are used, the attitude and bias observabilities can be highly improved because of the increase in geometrical variations.

(4) The current FHST calibration procedure depends on the attitude obtained from FPSS and hence provides no calibration in the roll direction. In fact, it may be possible to calibrate FHST independent of FPSS if proper slew maneuvers are performed within the mission contraints. It is important to calibrate the roll alighment of FHST because this is the only sensor which provides the roll information.

2.3 INERTIAL REFERENCE GYROS

2.3.1 Calibration Procedures and Results

The gyro assembly in IRU consists of three two-axis gyros. The outputs from three of the six axes are used in angular velocity calculations to specify the three components of the spacecraft's angular velocity vector. This angular velocity vector is then used to propagate the spacecraft attitude. Reliable gyro calibration is important to correctly measure the change in attitudes.

The gyro calibration function is performed by the Gyro Calibration Subsystem (CALIB) of SMM/ADS. A total of twelve calibration parameters are defined in CALIB. Nine of them form the 3x3 misalignment/scale factor correction matrix and the remaining three parameters give the gyro drift rate bias vector.

The calibration method used in CALIB is a least-squares technique which minimizes the difference between the propagated attitudes derived from gyro measurements and the reference attitudes determined from FPSS and FHST.

Slew maneuvers were performed to support the gyro calibrations. During the SMM mission, the gyro calibration activity was repeated along with the FHST and FPSS sensor calibrations. The results showed that the gyro calibration parameters so detemined depend heavily on the results of FPSS and FHST calibration.

2.3.2 Discussions and Comments

The strong dependence of the gyro calibration results on the FHST and FPSS calibrations indicates that the true gyro calibration parameters probably have not yet been reached. This is because the desired long maneuvers for the gyro calibration purpose were not achieved due to mission and operational constraints. Thus, the current gyro calibration results depend heavily on the attitude determination accuracies at both ends of the calibration slews. In fact, gyro measures the change in attitude which should be insensitive to the attitude uncertainties caused by systematic errors as long as the same sensor was used in determining the starting and ending attitudes. Thus, the gyro may be better calibrated if the attitudes at both ends of a calibration slew are determined from the same sensor. However, it is important to collect as many observations as possible to reduce the effect due to random errors.

2.4 FINE POINTING SUN SENSOR

2.4.1 Calibration Procedures and Results

The FPSS measures the projected Sun angles in the SMM xy and xz planes. These measurements are used in FADS

to determine the pitch and yaw angles of the attitude. To ensure that the accuracy of the FPSS readings over the instrument's field-of-view are consistent with the SMM mission requirements of ±5 arc-sec, the FPSS were calibrated in-flight by the FPSS Off-Null Calibration System (SMM/FOCS).

The FPSS calibration parameters consist of a set of eight transfer function coefficients for each of the two measured angles, α and β. A recursive least-square filter was used in SMM/FOCS to determine these parameters by minimizing the residuals between the pitch and yaw angles computed from the FPSS measurements and the corresponding reference angles obtained from gyro measurements for a set of slew maneuvers.

The following conclusions resulted from the FPSS calibration activities.

(1) The discrete slew data gave better results than the continuous slew data due to the preaveraging process perfromed on the latter which reduces the effect due to random errors.

(2) The FPSS calibration results depend on the accuracy of the gyro calibration.

(3) Good agreement between the attitude changes measured by gyro and by FPSS were obtained after the FPSS calibration.

2.4.2 Discussions and Comments

Since the FPSS calibration was based on the gyro measurements, the accuracy of the FPSS calibration depends heavily on the gyro accuracies. Good agreement between the attitude changes measured by gyro and by FPSS does not necessarily ensure good FPSS calibration. The cur-

rent FPSS calibration results can be improved if the gyro can be better calibrated as discussed in Section 2.3.2. Furthermore, many of the parameters attempted to be determined in the FPSS calibration are not really distinguishable. Actually, these parameters are obtained from power series expansions of some analytical expressions[5] and hence are not all independent parameters. They are actually functions of a few constants which carry certain physical meanings. Thus reducing the number of parameters to be determined and defining proper relationships among the FPSS coefficients are essential in improving the FPSS calibration. This is given in Section 4.

SECTION 3 - GENERALIZED CALIBRATION/VERIFICATION SYSTEM BASELINE

This section presents the generalized system baseline for spacecraft calibration/verification functions. Section 3.1 describes the major functions which can be defined from this baseline. Section 3.2 gives an overview of the algorithm to be used in the baseline and presents the baseline in terms of functional baseline and block diagrams. The external interfaces between subsystems and sample data file structures are also provided. Section 3.3 then summarizes the software modules required by each of the functions and outlines the modules which are sharable by different functions and missions.

3.1 MAJOR CALIBRATION/VERIFICATION FUNCTIONS

To ensure accurate attitude determination and control, three major activities related to sensor calibration are generally required by each mission. Namely, the prelaunch attitude and bias observability and data collection strategy studies; the in-flight sensor calibration and bias determinations; and the post-calibration attitude accuracy verifications.

The first function requires a predictor which predicts the attitude and sensor bias determination accuracies achievable under various geometrical conditions. This function is important because the results of these studies often can be used to enhance the sensor selections and configurations, to improve the mission timeline schedules, and to aid the data acquisition and maneuver plannings. Most of all, they provide the prelaunch knowledge of the attitude and sensor bias

determination accuracies achievable from each of the sensors at various geometrical conditions. This knowledge is essential in ensuring the fullfillment of the attitude accuracy requirements, optimizing the attitude determination and sensor calibration techniques and procedures, simplifying the operational supports, and improving the understanding of the realtime attitude and sensor bias determination results.

The second function requires a data processor which processes the realtime spacecraft data obtained from various sensors to determine the spacecraft attitudes and sensor biases. This sensor calibration activity is usually necessary to achieve the mission requirements on attitude determination and control accuracies. With the help of the predictor, data can be acquired under the most favorable conditions or from pre-scheduled maneuvers to optimize the bias observabilities. Since the sensor calibration function requires relatively long data spans, it is generally performed on ground with the results uplinked to the spacecraft. The onboard computer then determines the spacecraft attitudes momentarily using the calibrated sensors.

The third function requires a quality assurance system which compares the attitudes determined momentarily onboard with the attitudes obtained from the ground processing when sensors are recalibrated using long data spans. This serves as a verification of the validities of the sensor calibration results carried onboard. If the difference between the attitudes exceeds the attitude accuracy requirement, it indicates that the current sensor calibration information carried onboard needs updates and refinements. This verification function is important when the sensor biases are not truely constant.

3.2 SYSTEM BASELINE

This section presents the baseline of the generalized calibration/verification system (GCS). From this baseline, the system specifications for the three functions described in Section 3.1 can be defined. An overview of the algorithm to be used by GCS is given in Section 3.2.1. The functional baseline and block diagrams are presented in Section 3.2.2.

3.2.1 System Algorithm Overview

The theoretical basis of GCS is a least-squares filter which determines the elements of a "state vector" by minimizing the square of the difference between the observed data and the expected data computed from an observation model. Detailed descriptions, categorizations, and comparisons of least-squares filters can be found in Reference 5.

The following least-squares estimators are chosen for the implementation of GCS. In the case of an inertially fixed state, a "batch least-squares estimator" will be used which updates the state vector after processing a block of observations and iterates the state until a converged solution is obtained. In the case of dynamically varying states, a "Kalman filter" will be used to propagate the state from one time to the next. In a Kalman filter, the filter's confidence in its estimate of the state is allowed to degrade from one update to another using models of noise in the state vector. This causes the influence of earlier data on the current state to fade with time so that the filter does not lose sensitivity to current observations. A Kalman filter reduces to a "recursive least-squares estimator" when

the state noise is zero.

The mathematical formulations of the least-squares estimator used in GCS is summarized in the following. To update the state and covariance during an inertial state, equations for a batch least-squares estimator are used. That is

$$\underline{X}_k = \underline{X}_{k-1} + P_k \left[\sum_{\ell=0}^{n} (H^T R^{-1} \underline{v})_{t_\ell \underline{X}_{k-1}} + P_0^{-1} (\underline{X}_0 - \underline{X}_{k-1}) \right] \tag{3-1}$$

$$P_k = \left[P_0^{-1} + \sum_{\ell=0}^{n} (H^T R^{-1} H)_{t_\ell \underline{X}_{k-1}} \right]^{-1} \tag{3-2}$$

where

k = iteration number

$\underline{X}$ = state vector

P = covariance matrix

H = observation partial derivative matrix

R = observation error matrix

$\underline{v}$ = observation residual vector

ℓ = time index

To propagate the state and covariance for a dynamically varying state, equations for a Kalman filter are used. That is,

$$\underline{X}_{i+1} = \phi_i \underline{X}_i \tag{3-3}$$

$$P_{i+1} = \phi_i P_i \phi_i^T + \Gamma_i Q_i \Gamma_i^T \tag{3-4}$$

where

i = time index

$\underline{X}$ = state vector

P = covariance matrix

ϕ = state transition matrix

Q = state noise matrix

Γ = state noise transition matrix

The analytical expressions of the entries in Equations (3-1) to (3-4) for each of the observation and transition models will be given in Section 4.

Equations (3-1) to (3-4) are necessary for both calibration and verification functions where data processing capability is required. However, for an observability prediction system, only Equations (3-2) and (3-4) are needed. In this case, a nominal state will be assumed which either stays constant or propagates with time through given functional variations. Furthermore, a predictor does not require observation data. It only requires an observation model which predicts the times and uncertainties of the observations. These differences due to different functions are indicated in the baseline whenever necessary.

3.2.2 System Baseline and Block Diagrams

Figure 3-1 shows the functional baseline diagram of GCS and its external interfaces. GCS will operate under the Graphics Executive Support System (GESS) and use the core allocation/deallocation graphics displays and interactive processing services provided by this executive. The system contains four major parts: the main driver (DRIVER), the state initialization and data preparation subsystem (SIDP), the state and covariance update and propagation subsystem (FILTR), and the attitude verification subsystem (VERIF). The functional block diagrams of these four parts are shown in Figures (3-2) to (3-5). In these figures, software modules which can

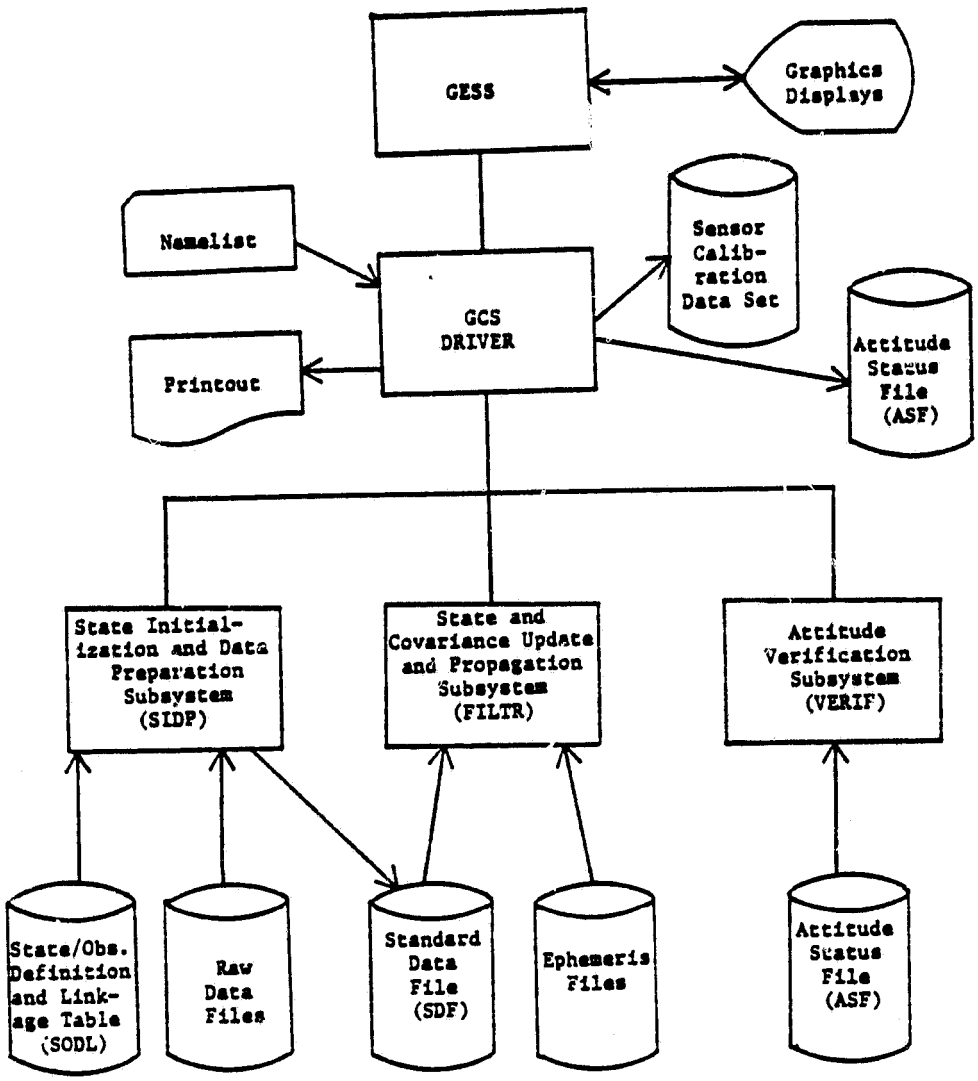

Figure 3-1. Functional Baseline Diagram of GCS

be applied in general to all missions and sensors are enclosed by solid boxes and those modules which are mission or sensor dependent are enclosed with dashed boxes.

The primary functions of the DRIVER is to handle inputs/outputs and to serve as a linkage between the GESS executive and the three subsystems of GCS. It reads the input parameters through either cards or graphic terminals. The outputs can lead to the lineprinters, the graphic terminals, or the disc data files. Two disc data files can be updated by DRIVER as a result of the attitude and bias determination: the Sensor Calibration Data Set which stores the updated sensor calibration parameter, and the Attitude Status File which stores the attitude determination results.

The SIDP subsystem is responsible for the state and covariance initializations and data preparations. To generalize the system, a State/Observation Definition and Linkage File (SODL) is required to define the observation and transition models included in the system and to link each model with its related state elements. A sample file structure for SODL is shown in Table 3-1. With SODL, the system will automatically define the corresponding state vector elements for the user once a given combination of observation and transition models are selected.

After the state vector is defined, and the initial covariance and state are acquired, SIDP then creates a Standard Data File (SDF) from the individual raw data files or from given data modelings. The SDF has a standard file structure which is required by the FILTR subsystem. Briefly, it combines various observation and

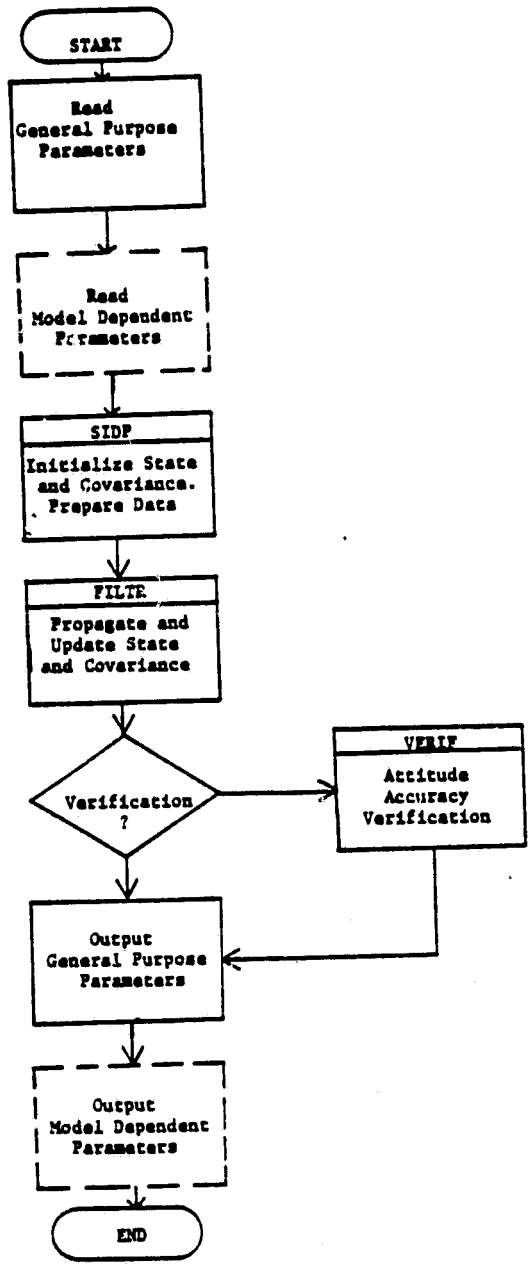

Figure 3-2. Functional Block Diagram of GCS/DRIVER

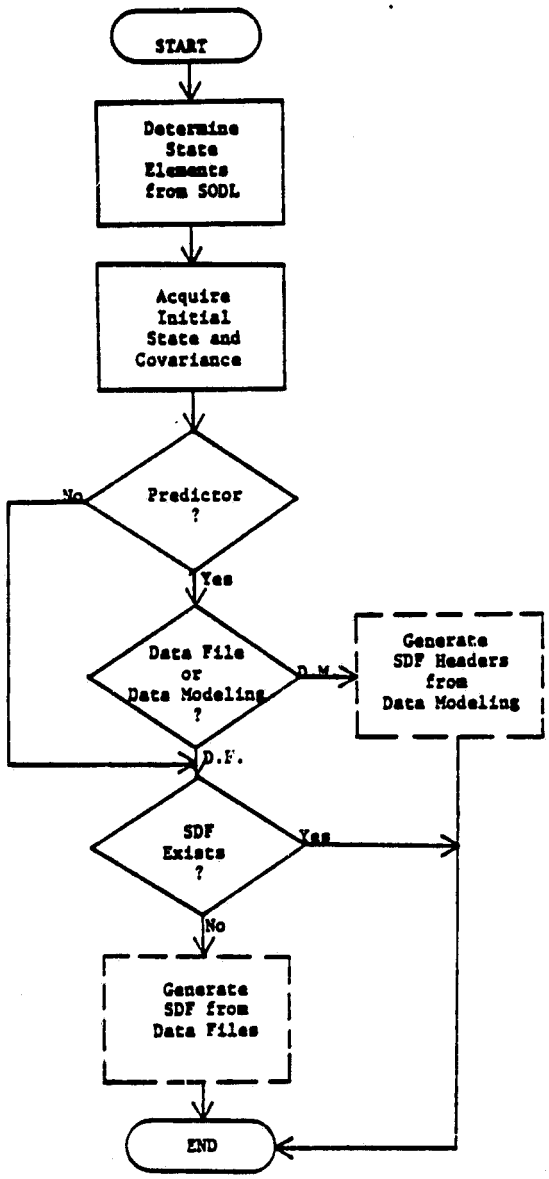

Figure 3-3. Functional Block Diagram of GCS/SIDP

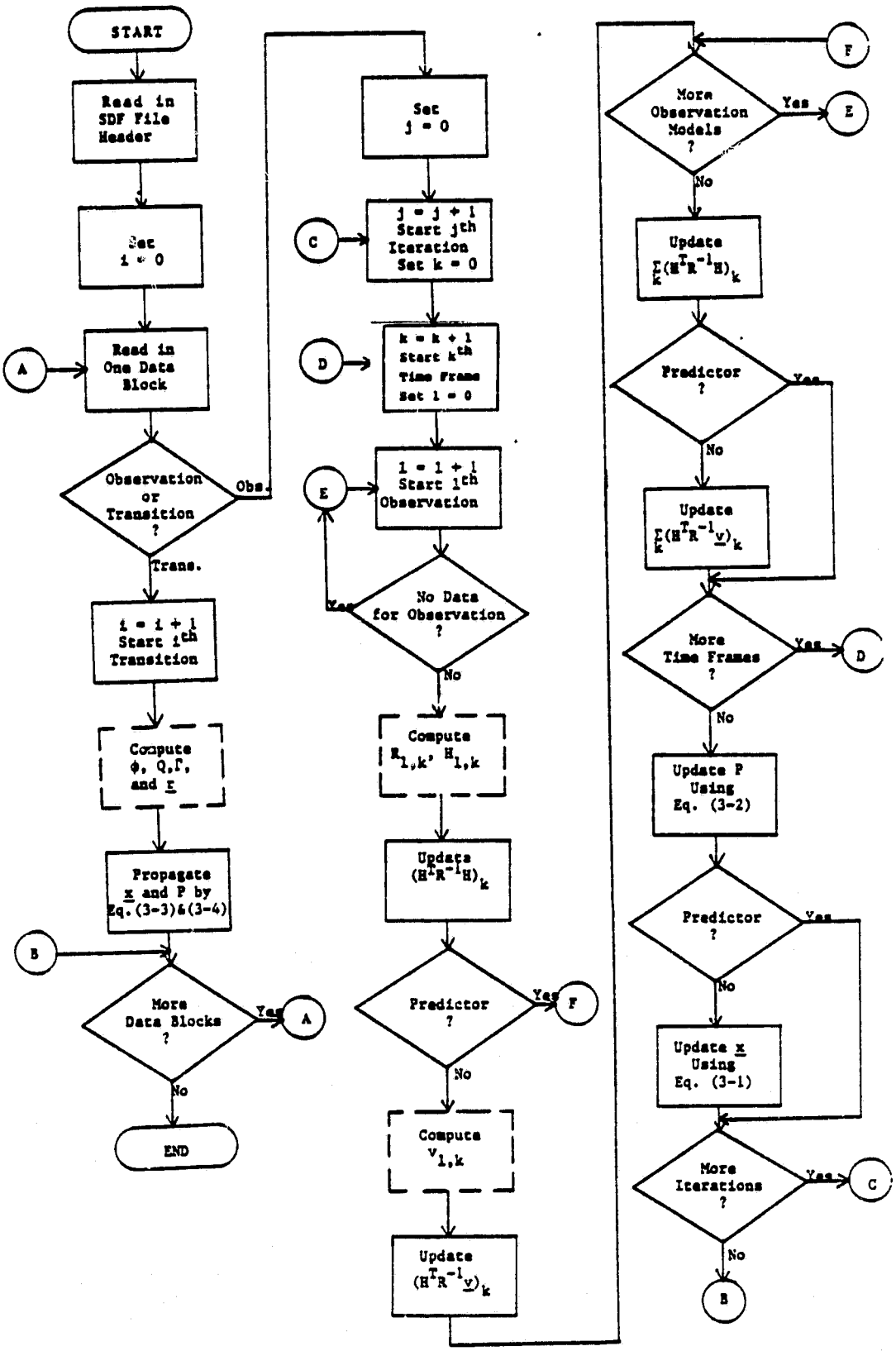

Figure 3-4. Functional Block Diagram of GCS/FILTR

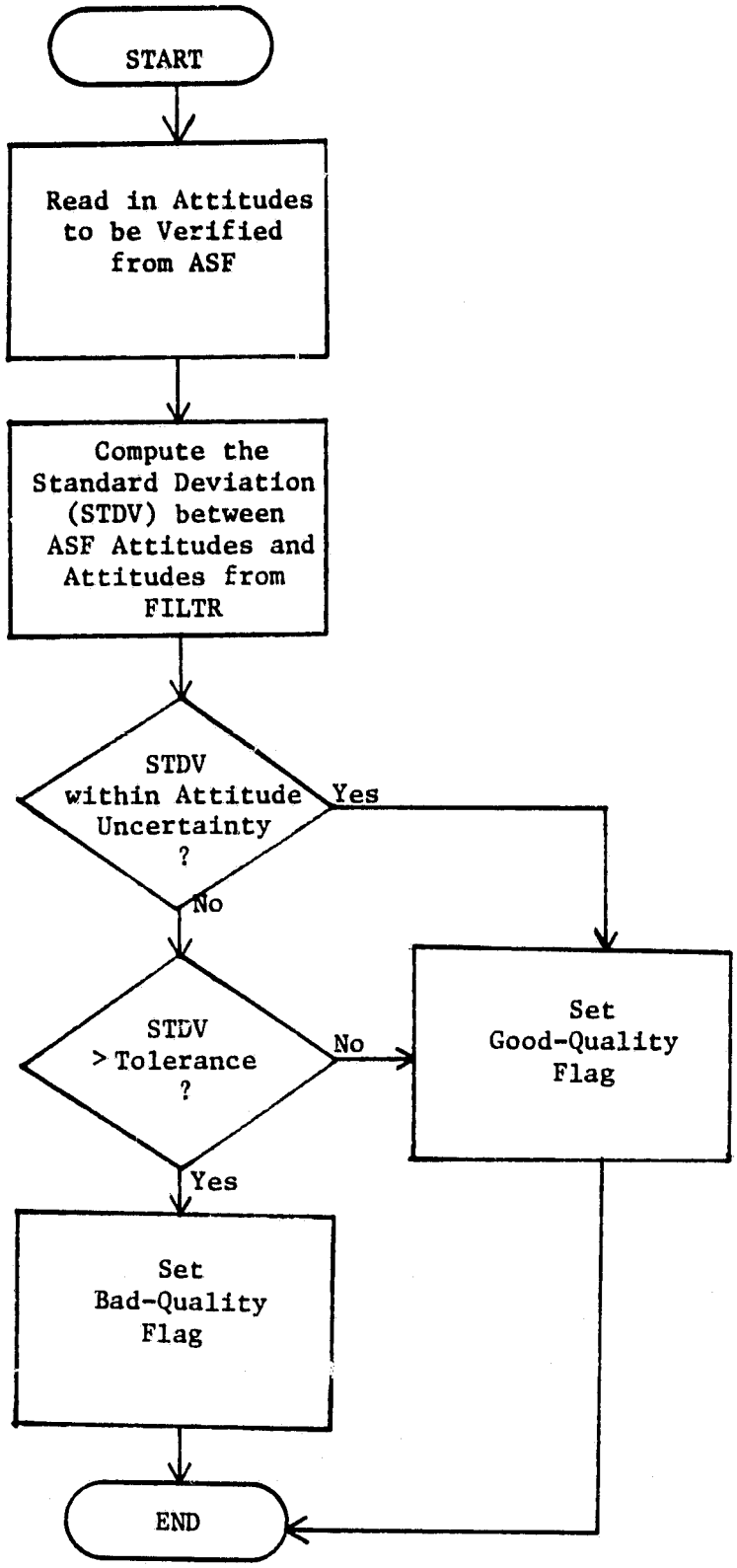

Figure 3-5. Functional Block Diagram of GCS/VERIF

Table 3-1. Sample File Structure of SODL

Record Number	Record Description	Word Number	Word Description
1	Observation model header	1	Total number of observation models
		2-3	Name of observation model 1
		4	Record number of the information record for observation 1
		5 on	Repeat words 2-4 for other observation models
2	Transition model header	1	Total number of transition models
		2-3	Name of transition model 1
		4	Record number of the information record for transition 1
		5 on	Repeat words 2-4 for other transition models
3	State element header	1	Total number of state elements
		2-3	Name of state element 1
		4 on	Repeat words 2-3 for other state elements
4	Information record for Observation 1	1	Total number of state elements related to this observation
		2	State element ID of the first related element
		3 on	Repeat word 2 for other related state elements
5	Repeat Record 4 for other obs.		

transition data into data blocks. Each data block is identified as either an observation block which measures an inertial state, or a transition block which measures the state transitions. A sample SDF structure is shown in Table 3-2. In the case of a predictor, the state observabilities can be predicted either from actual data or from some data modelings. In the latter case, only the header information of SDF, which gives the time and the amount of data, needs to be generated. There is no need of simulating the actual data content.

The FILTR subsystem is the center of GCS. It reads the data from SDF and performs all the necessary computations to optimize the state and determine the covariance. It processes one block of data at a time. Equations (3-1) and (3-2) are used to process the observation data blocks and Equations (3-3) and (3-4) are used to process the transition data blocks. The state is updated after each observation processing and propagated after each transition processing. The batch least-squares filter of each observation block contains only a single time frame and only one iteration is performed on each data processing.

In the case of a predictor, the state will be kept at its nominal values and only the covariance matrix needs to be updated and propagated.

The VERIF subsystem is required by the verification function only. It reads in the attitudes to be verified from the attitude status file, compares these attitudes with the attitudes obtained from FILTR when the updated sensor calibration parameters are used and sends an indication flag when the difference is greater than the attitude accuracy requirement.

3.3 SUMMARY OF SOFTWARE MODULES

A summary of functional software modules required by GCS is given in Table 3-3. For each of the modules, Table 3-3 specifies the functions by which the module is required and indicates if the module is mission or sensor dependent. This provides a guideline of the amount of software sharable by different missions and functions if the generalized calibration/verification system is implemented.

Table 3-2. Sample File Structure of SDF

Record Number	Record Description	Word Number	Word Description
1	File Header	1	Total number of data blocks
		2	File Type (1= headers + data, 2= headers only)
2	Header of 1st data block	1	Block ID (1= observation, 2= transition)
		2	Number of time frames in the block
3	Header of 1st time frame in the block	1-2	Frame time
		3	Number of data record in the frame
		4	Number of data points in model 1
		5 on	Repeat word 4 for other models
4 to n	Data records of 1st time frame in the block		
n+1 to n	Repeat records 3 to n for other time frames in the block		
m+1 to end	Repeat records 2 to m for other data blocks		

Table 3-3. Summary of Functional Software Modules

Subsystem	Functional Software Module	Required by			Model Dependent
		Prediction	Calibration	Verification	
DRIVER	GESS and other external interfaces	X	X	X	No
	I/O of general purpose parameters	X	X	X	No
	I/O of model dependent parameters	X	X	X	Yes
SIDP	State element determination from SODL	X	X	X	No
	State and covariance initialization	X	X	X	No
	SDF generalization from raw data files		X	X	Yes
	SDF header generation from data modeling	X			Yes
FILTR	SDF Read	X	X	X	No
	Least-squares filter central processing	X	X	X	No
	State and covariance update and propagation	X	X	X	No
	Observation error and partial derivative matrices computations	X	X	X	Yes
	Observation residual computation		X	X	Yes
	State and covariance transition matrices computations	X	X	X	Yes
VERIF	ASF read			X	No
	Attitude computations			X	No

SECTION 4 - ANALYTICAL CONSIDERATIONS

This section presents the analytical equations required by the Generalized Calibration/Verification System (GCS) described in Section 3. Three types of attitudes are considered: (1) the single-axis spin-stabilized spacecraft, (2) the inertially-fixed three-axis spacecraft, and (3) the reference-pointing three-axis spacecraft. In the case of the single-axis spin-stabilized spacecraft, the attitude is defined by the orientation of the spin-axis which is inertially fixed. To determine such an attitude, the plane-field Sun sensor which measures the Sun angle, and the Earth horizon sensor which measures the time between the Sun-sighting event and the Earth horizon-crossing event are usually used. In the case of the three-axis stabilized spacecraft, the attitude is defined by the orientation between the spacecraft body axes and some reference axes. The sensors required for three-axis attitude determination typically include the coarse and fine two-axis digital Sun sensors, the three-axis magnetometers, the fixed-head Star trackers, and the inertial reference gyros.

Section 4.1 gives a general description of the coordinate system and attitude definitions to be used in the section. The transformation between different attitude representations, the modeling of attitude maneuvers, and the computation of spacecraft spin rate for reference-pointing spacecrafts are also given in Section 4.1. Section 4.2 provides the analytical considerations for each of the seven sensor types mentioned above. For each sensor type, the following subjects will be covered to include the necessary equations required by GCS: the

observation modeling, the state element definition, the nominal state, and the observation partial derivatives with respect to the state elements. For the case of gyros, equations required to perform state transitions and covariance propagations are also included. Section 4.3 discusses the estimation of observation errors and the data modeling for a prediction system. Section 4.4 describes the criterium used in attitude verification.

4.1 COORDINATE SYSTEMS AND ATTITUDE DEFINITIONS

4.1.1 Coordinate Systems

For the purpose of spacecraft attitude determination and sensor calibration, four types of coordinate systems are frequently used. These are: (1) the geocentric inertial (GCI) coordinate, (2) the body-fixed coordinate, (3) the reference coordinate, and (4) the sensor coordinate.

The GCI coordinate is fixed in the inertial space with x-axis pointing to the vernal equinox and the z-axis pointing to the celestial north pole. The body-fixed coordinate is a coordinate system which is fixed in the spacecraft body reference frame. The reference coordinate is needed for reference-pointing three-axis spacecrafts only. It is a coordinate system defined by the orientation of the reference body. For example, the axes of the reference coordinate, $(\hat{Q},\hat{\Diamond},\hat{W})$ of an Earth-pointing spacecraft expressed in the GCI coordinate is defined by

$$\begin{aligned} \hat{W} &= \underline{R}/|\underline{R}| \quad = \text{local vertical} \\ \hat{\Diamond} &= \hat{W} \times \underline{V}/|\hat{W} \times \underline{V}| \\ \hat{Q} &= \hat{\Diamond} \times \hat{W}/|\hat{\Diamond} \times \hat{W}| \end{aligned} \tag{4-1}$$

where $\underline{R}$ and $\underline{V}$ are the spacecraft position and velocity

vectors respectively. All vectors in Eq. (4-1) are expressed in the GCI coordinate. The reference coordinate for a Sun-pointing spacecraft such as SMM is defined by the SUN-coordinate as given in Reference 1. In general, the reference coordinate is not fixed inertially. The time variation of the reference frame is obtained from the ephemeris information. The sensor coordinate is defined by the sensor hardware mounted on the spacecraft. The orientation between the sensor coordinate and the body coordinate is usually described by an alignment matrix. Refinement of this alignment matrix is one of the major objectives of the in-flight spacecraft sensor calibrations.

In the rest of the document, a vector expressed in these four coordinate systems will be subscribed by I, B, R, and S respectively. Vectors without subscript are assumed to be expressed in the GCI coordinate.

4.1.2 Attitude Definitions

The definitions of attitudes for the single-axis and three-axis spacecrafts are given in the following subsections.

4.1.2.1 Single-Axis Attitude

The single-axis attitude is defined by the right ascension and declination of the spacecraft spin axis in the GCI coordinate. That is,

$$\hat{A} = \cos\alpha \cos\delta \, \hat{X}_I + \sin\alpha \cos\delta \, \hat{Y}_I + \sin\delta \, \hat{Z}_I \quad (4\text{-}2)$$

where

$\hat{A}$ = unit vector along the spin-axis

$\hat{X}_I$, $\hat{Y}_I$, $\hat{Z}_I$ are the three unit vectors in GCI coordinate

α = the right ascension of attitude

δ = the declination of attitude

4.1.2.2 Three-Axis Attitude

The three-axis attitude is in general defined by the orientation of the spacecraft body coordinate relative to the reference coordinate. This orientation can be represented by a coordinate transformation from the reference coordinate to the body coordinate as given below.

$$\underline{r}_B = [B]\ \underline{r}_R \tag{4-3}$$

where $\underline{r}_B$ and $\underline{r}_R$ corresponds to any vector $\underline{\gamma}$ represented in body and reference coordinates respectively. The matrix [B] which defines the attitude is generally expressed in terms of Euler angles.[5] Different conventions have been used in defining the Euler angle representations of attitudes. To standardize the attitude definition for GCS, the roll (ϕ), pitch (θ), and yaw (ψ) angles of an attitude are defined as the 1-2-3 Euler rotation angles of B . That is,

$$[B] = T_3(\psi)T_2(\theta)T_1(\phi) \tag{4-4}$$

$$= \begin{bmatrix} \cos\psi & \sin\psi & 0 \\ -\sin\psi & \cos\psi & 0 \\ 0 & 0 & 1 \end{bmatrix} \begin{bmatrix} \cos\theta & 0 & -\sin\theta \\ 0 & 1 & 0 \\ \sin\theta & 0 & \cos\theta \end{bmatrix} \begin{bmatrix} 1 & 0 & 0 \\ 0 & \cos\phi & \sin\phi \\ 0 & -\sin\phi & \cos\phi \end{bmatrix}$$

The Euler angles can be determined from the components of [B] by the following equation.

$$\begin{aligned} \phi &= \tan^{-1}\ (-B_{32}/B_{33}) && 0 \le \phi \le 2\pi \\ \theta &= \sin^{-1}\ (B_{31}) && -\tfrac{\pi}{2} \le \theta \le \tfrac{\pi}{2} \\ \psi &= \tan^{-1}\ (-B_{21}/B_{11}) && 0 \le \psi < 2\pi \end{aligned} \tag{4-5}$$

Another frequently used representation for three-axis attitude is the quaternion representation.[5] The quaternion representation does not involve trigonometric func-

tions and therefore is convenient to use in computations. Also because it carries simple product rule for successive rotations, the quaternion representation is usually used in computing the attitude transitions. In most practice, the quaternion representation of attitude is used to express the orientation of the spacecraft body coordinate relative to the GCI coordinate. That is,

$$\begin{aligned} \underline{r}_B &= [B]\ \underline{r}_R \\ &= [B][A]\underline{r}_I \\ &= [C(\bar{q})]\underline{r}_I \end{aligned} \tag{4-6}$$

where $[B]$ = the transformation matrix from reference coordinate to body coordinate as given in Eq. (4-4)

$[A]$ = the transformation matrix from the GCI coordinate to the reference coordinate

$[C]$ = the transformation matrix from the GCI coordinate to the body coordinate

$\bar{q}$ = $[\underline{q}, q_4]^T$ is the quaternion corresponding to the matrix $[C]$.

The matrix $[A]$ can be obtained from the ephemeris information by the following:

$$[A] = [I] \quad \text{for inertial-pointing spacecraft}$$

$$= \begin{bmatrix} \hat{u}_I^T \\ \hat{v}_I^T \\ \hat{w}_I^T \end{bmatrix} \quad \text{for reference-pointing spacecraft} \tag{4-7}$$

where $\hat{u}_I$, $\hat{v}_I$, $\hat{w}_I$ are the three unit axis vectors of the reference coordinate expressed in the GCI coordinate. The expression of [C] in terms of the quaternion is given by

$$\left[C(\bar{q})\right] = \begin{bmatrix} q_1^2-q_2^2-q_3^2+q_4^2 & 2(q_1q_2+q_3q_4) & 2(q_1q_3-q_2q_4) \\ 2(q_1q_2-q_3q_4) & -q_1^2+q_2^2-q_3^2+q_4^2 & 2(q_2q_3+q_1q_4) \\ 2(q_1q_3+q_2q_4) & 2(q_2q_3-q_1q_4) & -q_1^2-q_2^2+q_3^2+q_4^2 \end{bmatrix} \quad (4\text{-}8)$$

To determine the quaternion components in terms of the elements of [C], we have

$$\begin{aligned} q_4 &= \tfrac{1}{2}[1+C_{11}+C_{22}+C_{33}]^{\frac{1}{2}} \\ q_3 &= \frac{1}{4q_4}[C_{12}-C_{21}] \\ q_2 &= \frac{1}{4q_4}[C_{31}-C_{13}] \\ q_1 &= \frac{1}{4q_4}[C_{23}-C_{32}] \end{aligned} \quad (4\text{-}9a)$$

where

$$q_1^2+q_2^2+q_3^2+q_4^2 = 1 \quad (4\text{-}9b)$$

The quaternions carry a convenient product rule for successive rotations. Namely, if

$$[C(\bar{q}'')] = [C(\bar{q}')][C(\bar{q})] \quad (4\text{-}10a)$$

then

$$\bar{q}'' = \bar{\bar{q}}\bar{q}'$$

$$= \begin{bmatrix} q_4'q_3'-q_2'q_1' \\ -q_3'q_4' \; q_1'q_2' \\ q_2'-q_2'q_4'q_3' \\ -q_1'-q_2'-q_3'q_4' \end{bmatrix} \bar{q} \qquad (4\text{-}10b)$$

If both Euler angle and quaternion representations are used for the same transformation matrix, the Euler angles can be obtained directly from the quaternion components by[1]

$$\phi = \tan^{-1}\left[\frac{-2q_2q_3+2q_1q_4}{-q_1^2-q_2^2+q_3^2+q_4^2}\right] \qquad 0 \le \phi \le 2\pi$$

$$\theta = \sin^{-1}\left(2q_1q_3+2q_2q_4\right) \qquad -\frac{\pi}{2} \le \theta \le \frac{\pi}{2} \qquad (4\text{-}11)$$

$$\psi = \tan^{-1}\left[\frac{-2q_1q_2+2q_3q_4}{q_1^2-q_2^2-q_3^2+q_4^2}\right] \qquad 0 \le \Psi < 2\pi$$

4.2 ANALYTICAL CONSIDERATIONS FOR ATTITUDE SENSORS

The analytical equations required by GCS are given in the following subsections for each of the seven sensor types of concern, namely, the Earth horizon sensor, the plane-field Sun sensor, the coarse two-axis digital Sun sensor, the fine two-axis digital Sun sensor, the three-axis magnetometer, the fixed-head star tracker, and the inertial reference gyro. The first two sensor types are applied to the single-axis spacecrafts, while the remaining five sensor types are used for the three-axis spacecrafts. Detailed descriptions of these sensors and their modelings can be found in Reference 5.

4.2.1 Earth Horizon Scanners

The Earth horizon scanners measure the time durations between the Sun-sighting event and Earth horizon crossing events for the spinning spacecrafts. The equations for the sensor modeling and partial derivatives are summarized in the following. Detailed derivation of equations for the Earth horizon scanners can be found in Reference 6.

The analytical expression for the horizon-in/out time model is given by

$$y = \frac{1}{\omega}(\phi - \phi_H - \Delta\phi - \Delta\phi_s + \Delta\phi_H + 2\pi n) \quad n=0,\pm 1 \qquad (4\text{-}12a)$$

where

ω = spacecraft spin rate

ϕ = Sun to horizon-in/out dihedral angle

$$= \tan^{-1}\left[\frac{\hat{A}\cdot(\hat{S}\times\hat{H})}{\hat{S}\cdot\hat{H} - (\hat{S}\cdot\hat{A})(\hat{H}\cdot\hat{A})}\right] \qquad (4\text{-}12b)$$

$\hat{A}$ = spin axis attitude as given by Eq. (4-2)

$\hat{S}$ = Sun unit vector

$\hat{H}$ = unit vector along horizon line of sight at horizon-in/out time

$$= \cos(\rho+\Delta\rho)\hat{E} + \sin(\rho+\Delta\rho)(\hat{M}\sin\Lambda + \hat{N}\cos\Lambda) \qquad (4\text{-}12c)$$

$\hat{E}$ = nadir vector

$\hat{M} = \hat{A} \times \hat{E}/\sin\eta$ (η=nadir angle)

$\hat{N} = \hat{E} \times \hat{M}$

$$\cos\Lambda = \frac{\cos(\gamma+\Delta\gamma) - \cos(\rho+\Delta\rho)\cos\eta}{\sin(\rho+\Delta\rho)\sin\eta} \quad \begin{matrix}\text{'+' for horizon-out,}\\ \text{'-' for horizon-in)}\end{matrix}$$

where γ=sensor mounting angle

$\Delta\gamma$=sensor moutning angle bias

ρ=angular radius of Earth

$\Delta\rho$= bias on angular radius of Earth

$\sin \Lambda = \pm(1-\cos^2 \Lambda)^{\frac{1}{2}}$ ('+' for horizon-out,'-' for in)

ϕ_H = azimuth mounting angle between Sun sensor and horizon sensor

$\Delta\phi$ = constant azimuth bias due to mounting error or electronic delay

$\Delta\phi_s$ = azimuth error due to Sun sensor plane tilt

$= \sin^{-1} (\cot \beta \tan \varepsilon_s)$ (4-12d)

where β=Sun angle

s=Sun sensor plane tilt

$= \sin^{-1}[\cot(\gamma+\Delta\gamma) \tan \varepsilon_H]$ (4-12e)

where ε_H=Earth sensor plane tilt

Thus, the state vector for the Earth horizon-in/out model can be defined as the following.

$$\underline{X} = (\gamma, \delta, \Delta\phi, \Delta\gamma, \Delta\rho, \varepsilon_s, \varepsilon_H, \omega, \Delta t)^T \quad (4\text{-}13)$$

where Δt is the orbit in-track time error.

The equations for the partial derivatives of the observation with respect to the state elements are summarized in the following:

$$\frac{\partial y}{\partial \alpha} = \frac{1}{\omega} \left(\frac{\partial \phi}{\partial \alpha} - \sec\Delta\phi_s \csc^3 \beta \tan\varepsilon_s \hat{S} \cdot \frac{\partial \hat{A}}{\partial \alpha}\right)$$

$$\frac{\partial y}{\partial \delta} = \frac{1}{\omega} \left(\frac{\partial \phi}{\partial \beta} - \sec \Delta\phi_s \csc^3\beta \tan\varepsilon_s \hat{S} \cdot \frac{\partial \hat{A}}{\partial \delta}\right)$$

$$\frac{\partial y}{\partial \Delta\phi} = -\frac{1}{\omega}$$

$$\frac{\partial y}{\partial \Delta\gamma} = \frac{1}{\omega} \left[\frac{\partial \phi}{\partial \Delta\gamma} - \sec \Delta\phi_H \csc^3(\gamma+\Delta\gamma) \sin\varepsilon_H \sin(\gamma+\Delta\gamma)\right]$$

$$\frac{\partial y}{\partial \rho} = \frac{1}{\omega} \frac{\partial \phi}{\partial \Delta\rho}$$

$$\frac{\partial y}{\partial \varepsilon_S} = -\frac{1}{\omega} \sec\Delta\phi_S \cot\beta \sec^2 \varepsilon_S$$

$$\frac{\partial y}{\partial \varepsilon_H} = \frac{1}{\omega} \left\{ \frac{\partial \phi}{\partial \varepsilon_H} + \sec \Delta\phi_H \left[\cot(\gamma+\Delta\gamma) \sec^2 \varepsilon_H - \tan \varepsilon_H \csc^3(\gamma+\Delta\gamma) \sin \varepsilon_H \cos(\gamma+\Delta\gamma) \right] \right\}$$

$$\frac{\partial y}{\partial \omega} = \frac{-Y}{\omega}$$

$$\frac{\partial y}{\partial \Delta t} = \frac{1}{\omega} \frac{\partial \phi}{\partial \Delta t}$$

where

$$\frac{\partial \phi}{\partial x_i} = \frac{1}{1+\left(\frac{Q_1}{Q_2}\right)^2} \left(\frac{1}{Q_2} \frac{\partial Q_1}{\partial x_i} - \frac{Q_1}{Q_2^2} \frac{\partial Q_2}{\partial x_i} \right)$$

$$Q_1 = \hat{A} \cdot (\hat{S} \times \hat{H})$$

$$Q_2 = \hat{S} \cdot \hat{H} - (\hat{S} \cdot \hat{A})(\hat{H} \quad \hat{A})$$

$$\frac{\partial Q_1}{\partial x_i} = (\hat{S} \times \hat{H}) \cdot \frac{\partial \hat{A}}{\partial x_i} + (\hat{A} \times \hat{S}) \cdot \frac{\partial \hat{H}}{\partial x_i}$$

$$\frac{\partial Q_2}{\partial X_i} = \hat{S} \cdot \frac{\partial \hat{H}}{\partial x_i} - (\hat{H} \cdot \hat{A})(\hat{S} \cdot \frac{\partial \hat{A}}{\partial x_i})$$

$$+ (\hat{S} \cdot \hat{A}) \left[\sin(\gamma+\Delta\gamma) \cos \varepsilon_H \frac{\partial \Delta\gamma}{\partial x_i} + \cos(\gamma+\Delta\gamma) \sin \varepsilon_H \frac{\partial \varepsilon_H}{\partial x_i} \right]$$

$$\frac{\partial \hat{A}}{\partial x_i} = \hat{X}_I - \frac{A_1}{A_3} \hat{Z}_I \quad (\text{if } x_i = \alpha)$$

$$= \hat{Y}_I - \frac{A_2}{A_3} \hat{Z}_I \quad (\text{if } x_i = \delta)$$

$$= 0 \quad (\text{otherwise})$$

$$\frac{\partial \Delta\gamma}{\partial x_i} = 1 \quad (\text{if } x_i = \Delta\gamma)$$

$$= 0 \quad (\text{otherwise})$$

$$\frac{\partial \varepsilon_H}{\partial x_i} = 1 \quad (\text{if } x_i = \varepsilon_H)$$

$$= 0 \quad (\text{otherwise})$$

The partial derivatives of the horizon crossing vector with respect to the state elements, $\partial H/\partial x_i$, can be obtained by the following.

$$\frac{\partial \hat{H}}{\partial \alpha} = \frac{\hat{H} \times \hat{E}\left(\hat{H} \cdot \frac{\partial \hat{A}}{\partial \alpha}\right)}{\hat{E} \cdot (\hat{H} \times \hat{A})}$$

$$\frac{\partial \hat{H}}{\partial \delta} = \frac{\hat{H} \times \hat{E}\left(\hat{H} \cdot \frac{\partial \hat{A}}{\partial \delta}\right)}{\hat{E} \cdot (\hat{H} \times \hat{A})}$$

$$\frac{\partial \hat{H}}{\partial \Delta\gamma} = \frac{\hat{H} \times \hat{E} \sin(\gamma+\Delta\gamma)\cos \varepsilon_H}{\hat{E} \cdot (\hat{H} \times \hat{A})}$$

$$\frac{\partial \hat{H}}{\partial \Delta\rho} = \frac{\hat{H} \times \hat{A} \sin(\rho+\Delta\rho)}{\hat{E} \cdot (\hat{A} \times \hat{H})}$$

$$\frac{\partial \hat{H}}{\partial \varepsilon_H} = \frac{\hat{H} \times \hat{E} \cos(\gamma+\Delta\gamma)\sin \varepsilon_H}{\hat{E} \cdot (\hat{H} \times \hat{A})}$$

$$\frac{\partial \hat{H}}{\partial \Delta t} = \frac{\hat{A} \times \hat{H}}{\hat{E} \cdot (\hat{A} \times \hat{H})} \left[\left(\hat{H} - \hat{E} \frac{\cos\Delta\rho}{\cos\rho}\right) \cdot \underline{V}\right]$$

where $\underline{V}$ is the spacecraft velocity.

Two other observation models are oftenly used for the Earth horizon scanners, namely, the "Earth-width" model (y_w) and the "Sun to Earth mid-scan time" model (y_m). The former models the time span between the horizon-in and horizon-out events and the latter models the average of the Sun to horizon-in time and the Sun to horizon-out time. The partial derivatives for these two models are given by

$$\frac{\partial Y_w}{\partial x_i} = \frac{\partial Y_o}{\partial x_i} \quad \frac{\partial y_I}{\partial x_i}$$

$$\frac{\partial y_M}{\partial x_i} = \tfrac{1}{2}\left(\frac{\partial y_I}{\partial x_i} + \frac{\partial y_O}{\partial x_i} \right)$$

where y_I and y_O are the Sun to horizon-in time and Sun to horizon-out time models respectively and x_i are the state elements.

4.2.2 Plane-Field Sun Sensor

The plane-field Sun sensor measures the Sun angle (β) between the Sun-vector and the spacecraft spin axis. It is usually used in conjunction with the Earth horizon sensors to determine the spacecraft attitudes for single-axis spacecrafts. The sensor modeling and partial derivatives are summarized below.

The Sun angle model for the plane-field Sun sensor is defined by the following

$$y = \cos^{-1}(\cos\beta \sec \varepsilon_s) - \Delta\beta \qquad (4\text{-}14)$$

where β is the Sun angle, ε_s is the Sun sensor plane tilt, and $\Delta\beta$ is the Sun angle bias. The state vector for this observation model is thus defined by

$$\underline{x} = (\alpha, \delta, \Delta\beta, \varepsilon_s)^T \qquad (4\text{-}15)$$

The partial derivatives of the observation with respect to the state elements are

$$\frac{\partial y}{\partial \alpha} = \chi(A_2 S_1 - A_1 S_2)$$

$$\frac{\partial y}{\partial \delta} = \frac{\chi}{\sqrt{1-A_3^2}} (\cos\beta\, A_3 - S_3)$$

$$\frac{\partial y}{\partial \Delta\beta} = 1$$

$$\frac{\partial y}{\partial \varepsilon_s} = -\chi \cos\beta \tan\varepsilon_s$$

where

$$\chi = \frac{1}{\sqrt{\cos^2\varepsilon_s - \cos^2\beta}}$$

4.2.3 Coarse Two-Axis Digital Sun Sensor

The coarse two-axis digital Sun sensor measures the projected Sun angles, α and β, in the xy and xz planes of the sensor coordinate. The measurements are related to these angles by the following:

$$y_\alpha = N_\alpha = \frac{1}{K_\alpha}(\alpha + b_\alpha) \qquad (4\text{-}16a)$$

$$y_\beta = N_\beta = \frac{1}{K_\beta}(\beta + b_\beta) \qquad (4\text{-}16b)$$

where K_α and K_β are the scale factors and b_α and b_β are the Sun agnle biases. Theα and β angles are related to the Sun vector by

$$\alpha = \tan^{-1}\left(\frac{S_{ys}}{S_{xs}}\right) \qquad (4\text{-}17a)$$

$$\beta = \tan^{-1}\left(\frac{S_{zs}}{S_{xs}}\right) \qquad (4\text{-}17b)$$

where S_{xs}, S_{ys}, and S_{zs} are the components of the unit Sun vector in the Sun sensor coordinate. To express $\hat{S}_s$ in terms of the attitude, we have

$$\hat{S}_s = [M][B]\hat{S}_R \qquad (4\text{-}18)$$

where [M] is the Sun sensor alignment matrix which transforms a vector from the spacecraft body coordinate to the sensor coordinate, [B] is a function of the Euler angles which defines the spacecraft attitude (Eq.(4-4)), and $\hat{S}_R$ is the Sun vector expressed in the reference coordinate which can be obtained from the ephemeris information using Equations (4-6) and (4-7). Thus, the Sun sensor measurements N_α and N_β are related to the Euler angles ϕ, θ, ψ through the Equations (4-16) to (4-18) and (4-4).

Assuming errors due to sensor misalignment are negligible, then the state vector for coarse two-axis Sun sensors can be defined as

$$\underline{X} = (\phi,\ \theta,\ \psi,\ K_i,\ b_i) \qquad i=\alpha,\ \beta \qquad (4\text{-}19)$$

The partial derivatives of the observation with respect to the state elements are given by

$$\frac{\partial y_i}{\partial k_i} = -\frac{y_i}{k_i} \quad (i=\alpha,\beta)$$

$$\frac{\partial y_i}{\partial b_i} = \frac{1}{k_i} \qquad (i=\alpha,\beta)$$

$$\frac{\partial y_i}{\partial x_j} = \frac{1}{k_\alpha}\left(\frac{\partial \alpha}{\partial x_j}\right) \qquad (x_j = \phi,\ \theta,\ \psi,)$$

$$\frac{\partial y_\beta}{\partial x_j} = \frac{1}{k_\beta}\left(\frac{\partial \beta}{\partial x_j}\right) \qquad (x_j = \phi,\ \theta,\ \psi,)$$

where

$$\frac{\partial \alpha}{\partial x_j} = \frac{1}{S_{xs}^2+S_{ys}^2}\left[S_{xs}\left(\frac{\partial S_{ys}}{\partial x_j}\right) - S_{ys}\left(\frac{\partial S_{ys}}{\partial x_j}\right)\right] \qquad (4\text{-}20a)$$

$$\frac{\partial \beta}{\partial x_j} = \frac{1}{S_{xs}^2+S_{zs}^2}\left[S_{xs}\left(\frac{\partial S_{zs}}{\partial x_j}\right)-S_{zs}\left(\frac{\partial S_{xs}}{\partial x_j}\right)\right] \qquad (4\text{-}20b)$$

and the partial derivatives of S with respect to the Euler angles are

$$\frac{\partial \hat{S}^s}{\partial x^j} = [M]\frac{\partial [B]}{\partial x^j}\hat{S}_R \qquad (4\text{-}21)$$

where

$$\frac{\partial [B]}{\partial \phi} = \begin{bmatrix}\cos\psi & \sin\psi & 0\\ -\sin\psi & \cos\psi & 0\\ 0 & 0 & 1\end{bmatrix}\begin{bmatrix}\cos\theta & 0 & -\sin\theta\\ 0 & 1 & 0\\ \sin\theta & 0 & \cos\theta\end{bmatrix}\begin{bmatrix}0 & 0 & 0\\ 0 & -\sin\phi & \cos\phi\\ 0 & -\cos\phi & -\sin\phi\end{bmatrix}$$

$$\frac{\partial [B]}{\partial \theta} = \begin{bmatrix}\cos\psi & \sin\psi & 0\\ -\sin\psi & \cos\psi & 0\\ 0 & 0 & 1\end{bmatrix}\begin{bmatrix}-\sin\theta & 0 & -\cos\theta\\ 0 & 0 & 0\\ \cos\theta & 0 & -\sin\theta\end{bmatrix}\begin{bmatrix}1 & 0 & 0\\ 0 & \cos\phi & \sin\phi\\ 0 & -\sin\phi & \cos\phi\end{bmatrix}$$

$$\frac{\partial [B]}{\partial \psi} = \begin{bmatrix}-\sin\psi & \cos\psi & 0\\ -\cos\psi & -\sin\psi & 0\\ 0 & 0 & 0\end{bmatrix}\begin{bmatrix}\cos\theta & 0 & -\sin\theta\\ 0 & 1 & 0\\ \sin\theta & 0 & \cos\theta\end{bmatrix}\begin{bmatrix}1 & 0 & 0\\ 0 & \cos\phi & \sin\phi\\ 0 & -\sin\phi & \cos\phi\end{bmatrix}$$

4.2.4 Fine Two-axis Digital Sun Sensor

Similar to the coarse Sun sensor, the fine Sun sensor also measures the α and β angles of the Sun vector. However, more parameters are included in the observation models to describe fine residuals in the measurement. As shown in Reference 5, the fine Sun sensor measurements can be modeled by the following expressions

$$Y_\alpha = N_\alpha = \frac{1}{A_2}\left[\tan\alpha - A_1 - A_3 \sin(k_\alpha \tan\alpha)\right] \qquad (4\text{-}23a)$$

$$Y_\beta = N_\beta = \frac{1}{B_2}\left[\tan\beta - B_1 - B_3 \sin(k_\beta \tan\beta)\right] \qquad (4\text{-}23b)$$

where A_i, B_i, k_α, and k_β are the sensor parameters to be calibrated. It can be shown that the following expressions for α and β in terms of N_α and N_β are obtained when proper iterative approximations are performed. That is,

$$\alpha = \tan^{-1}\left[A_1+A_2N_\alpha+A_3\sin(A_4N_\alpha+A_5)+A_6\sin(A_7N_\alpha+A_8)\right] \quad (4\text{-}24a)$$

$$\beta = \tan^{-1}\left[B_1+B_2N_\beta+B_3\sin(B_4N_\beta+B_5)+B_6\sin(B_7N_\beta+B_8)\right] \quad (4\text{-}24b)$$

In Equation (4-23), the high order coefficients are not independent parameters. They are related to the parameters in Eq. (4-22) by

$$\begin{aligned} A_4 &= k_\alpha A_2 & B_4 &= k_\beta B_2 \\ A_5 &= k_\alpha A_1 & B_5 &= k_\beta B_1 \\ A_6 &= k_\alpha A_3^2/2 & B_6 &= k_\beta B_3^2/2 \\ A_7 &= 2A_4 & B_7 &= 2B_4 \\ A_8 &= 2A_5 & B_8 &= 2B_5 \end{aligned} \quad (4\text{-}25)$$

The state vectors for the fine Sun sensor are defined as

$$\underline{X}_\alpha = (\phi,\theta,\psi,A_1,A_2,A_3,k_\alpha)^T \quad (4\text{-}26a)$$

$$\underline{X}_\beta = (\phi,\theta,\psi,B_1,B_2,B_3,k_\beta)^T \quad (4\text{-}26b)$$

The partial derivatives of Y_α are given below. Analogous expressions can be obtained for that of Y_β.

$$\frac{\partial Y_\alpha}{\partial A_1} = -\frac{1}{A_2}$$

$$\frac{\partial Y_\alpha}{\partial A_2} = -\frac{Y_\alpha}{A_2}$$

$$\frac{\partial Y_\alpha}{\partial A_3} \quad \frac{1}{A_2}\sin(k_\alpha \tan^\alpha)$$

$$\frac{\partial Y^{\alpha}}{k} = -\frac{A_3}{A_2}\cos(k_{\alpha}\tan\alpha)\tan\alpha$$

$$\frac{\partial Y^{\alpha}}{\partial x^{j}} = \frac{1}{A_2\cos^2\alpha}\left[1 - k_{\alpha}A_3\cos(k_{\alpha}\tan\alpha)\right]\frac{\partial\alpha}{\partial x^{j}}$$

where $x_j = \phi,\theta,\psi$ and $\partial\alpha/\partial x^j$ is given by Equations (4-20) to (4-22).

4.2.5 Three-Axis Magnetometer

The three-axis magnetometer measures the components of the geomagnetic field in the magnetometer frame, $\underline{H}_S$. The sensor observation can be modeled as

$$\underline{Y} = \underline{H}_S + \underline{b}$$

$$= [M]\ [B]\ [A]\ \underline{H}_I + \underline{b} \qquad (4\text{-}27)$$

where [M] is the magnetometer alignment matrix which transforms a vector from body coordinate to the magnetometer sensor coordinate, [B] and [A] are defined in Equations (4-4) and (4-7) respectively, $\underline{H}_I$ is the geomagnetic field in the GCI coordinate which can be computed from mathematical models of the geomagnetic field, and $\underline{b}$ is a constant bias vector on the magnetometer measurements.

Assuming the error due to sensor misalignment is negligible, then the state vector for the magnetometer observations can be defined as

$$\underline{X} = (\phi,\theta,\psi,\ \underline{b})^T \qquad (4\text{-}28)$$

The observation partial derivatives with respect to the state elements are given by

$$\frac{\partial y_i}{\partial b_j} = \delta_{ij}$$

$$\frac{\partial y}{\partial x_i} = [M] \frac{\partial [B]}{\partial x_i} [A] \underline{H}_I \qquad (i=1,2,3)$$

where $\partial[B]/\partial x_i$ is given in Eq. (4-22).

4.2.6 Fixed-Head Star Tracker

Analogous to the two-axis Sun sensors, the star tracker measures the direction of a given star in the tracker coordinate. The two measurements are related to the star direction by the following equations

$$y_H = \frac{1}{S_H} \sin^{-1} F_{Zs} \qquad (4\text{-}29a)$$

$$y_V = \frac{1}{S_V} \tan^{-1} \frac{F_{ys}}{F_{xs}} \qquad (4\text{-}29b)$$

where S_H and S_v are the scale factors and $\hat{F}_s = (F_{xs}, F_{ys}, F_{zs})^T$ is the unit star vector in the tracker coordinate. $\hat{F}_s$ can then be expressed in terms of the attitude parameters by

$$\hat{F}_s = [M][B][A]\,\hat{F}_I \qquad (4\text{-}30)$$

Here, [M] is the star tracker alignment matrix which transforms a vector from the body coordinate to the tracker coordinate, [B] and [A] are defined in Equations (4-4) and (4-7), and $\hat{F}_I$ is the unit star vector in the GCI coordinate which can be obtained from the star catalog. In order to calibrate the star tracker alignment, the matrix M can be expressed in terms of three rotation angles as following.

$$[M] = T_3(\delta)\, T_2(\beta)\, T_1(\alpha)$$

where T_1, T_2, T_3 are the rotation matrices defined in Equation (4-4). Thus, the state vector for the star tracker can be defined as

$$\underline{X} = (\phi,\theta,\psi,\alpha,\beta,\delta,s_H,s_V) \qquad (4\text{-}31)$$

The partial derivative equations for the star trackers are:

$$\frac{\partial y_H}{\partial s_H} = -\frac{y_H}{s_H}$$

$$\frac{\partial y_H}{\partial s_V} = 0$$

$$\frac{\partial y_V}{\partial s_V} = 0$$

$$\frac{\partial y_V}{\partial s_V} = -\frac{y_V}{s_V}$$

$$\frac{\partial y_H}{\partial x_i} = \frac{1}{s_H}\,\frac{1}{\sqrt{1-F^2}}\left(\frac{\partial F_z}{x_i}\right)$$

$$\frac{y_V}{x_i} = -\frac{1}{s_V}\,\frac{1}{F^2_{xs}+F^2_{ys}}\left[F_{xs}\left(\frac{\partial F_{ys}}{\partial x_i}\right)-F_{ys}\left(\frac{\partial F_{xs}}{}\right)\right]$$

where $x_i = \phi,\theta,\psi,\alpha,\beta,\delta$. The partial derivatives of F_s with respect to x_i are given by

$$\frac{\partial \hat{F}_s}{\partial X_i} = \frac{\partial [M]}{\partial X_i} \quad B][A]\,\hat{F}_I \qquad (\text{if } X_i = \alpha,\beta,\delta)$$

$$\frac{\partial \hat{F}_s}{\partial X_i} = [M]\,\frac{\partial [B]}{\partial X_i}[A]\,\hat{F}_I \qquad (\text{if } X_i = \phi,\theta,\psi)$$

where $\partial[B]/\partial X_i$ is given by Eq. (4-22). Similar Equations can be derived for $\partial[M]/\partial X_i$. That is,

$$\frac{\partial [M]}{\partial \alpha} = \begin{bmatrix} \cos\delta & \sin\delta & 0 & \cos\beta & 0 & -\sin\beta & 0 & 0 & 0 \\ -\sin\delta & \cos\delta & 0 & 0 & 1 & 0 & 0 & -\sin\alpha & \cos\alpha \\ 0 & 0 & 1 & \sin\beta & 0 & \cos\beta & 0 & -\cos\alpha & -\sin\alpha \end{bmatrix}$$

$$\frac{\partial [M]}{\partial \beta} = \begin{bmatrix} \cos\delta & \sin\delta & 0 & -\sin\beta & 0 & -\cos\beta & 1 & 0 & 0 \\ -\sin\delta & \cos\delta & 0 & 0 & 0 & 0 & 0 & \cos\alpha & \sin\alpha \\ 0 & 0 & 1 & \cos\beta & 0 & -\sin\beta & 0 & -\sin\alpha & \cos\alpha \end{bmatrix}$$

$$\frac{\partial [M]}{\partial \delta} \quad \begin{bmatrix} -\sin\delta & \cos\delta & 0 & \cos\beta & 0 & -\sin\beta & 1 & 0 & 0 \\ -\cos\delta & \sin\delta & 0 & 0 & 1 & 0 & 0 & \cos\alpha & \sin\alpha \\ 0 & 0 & 0 & \sin\beta & 0 & \cos\beta & 0 & -\sin\alpha & \cos\alpha \end{bmatrix}$$

4.2.7 Inertial Reference Gyro

The inertial reference gyros measure the spacecraft angular velocity relative to the inertial coordinate. This measurement can be used to compute the state transition and to propagate the covariance matrix. It can also be used as an observation to calibrate the gyros. These two functions are separately in the following subsections.

4.2.7.1 Gyro Calibration

The gyro measurements are related to the spacecraft angular velocity by the following relation:

$$\underline{Y} = [G] \ (\underline{\omega} + \underline{b}) \tag{4-32}$$

where $[G]$ is the inverse of the gyro scale factor correction and alignment matrix, $\underline{\omega}$ is the averaged spacecraft angular velocity over the gyro measurement frame, and $\underline{b}$ is the gyro drift rate bias. The angular velocity $\underline{\omega}$ can be determined from the initial and final attitudes using the quaternion representation. If $\bar{q}(t-\tau)$ and $\bar{q}(t)$ are the initial and final attitudes, then $\underline{\omega}$ is obtained from the following procedures.

$$\text{Let} \quad \bar{Q} = \bar{q}\,(t-\tau) * \bar{q}(t) = (\underline{Q}, Q_4)^T \tag{4-33a}$$

where $\bar{q}^*$ = the conjugate of $\bar{q}$
$= (-\underline{q}, q_4)^T$

then,

$$\underline{\omega} = \frac{\omega}{\sin(\frac{\tau}{2})} \ \underline{Q} \tag{4-33b}$$

where

$$\omega = \frac{2}{\tau} \cos^{-1} Q_4 \tag{4-33c}$$

Equation (4-33a) requires the quaternion multiplication which is given by Eq. (4-10b). For the case of observability predictions, the nominal spacecraft angular velocity can be obtained directly from the ephemeris in-

formation. The angular velocity for an Earth-pointing spacecraft is given by

$$\underline{\omega} = - \frac{\underline{V} \cdot \hat{u}}{R} \hat{v} \qquad (4\text{-}34)$$

where R is the distance between the spacecraft and the Earth, $\underline{V}$ is the spacecraft velocity, and $\hat{u}$, $\hat{v}$ are defined in Equation (4-1).

To model the attitude maneuvers starting from time t_0, the attitude at time t is given by

$$\left[C(\bar{q}_t)\right] = \left[B_t\right] \left[A_t\right] \qquad (4\text{-}35)$$

where A_t is given by the ephemeris and is given by Equation (4-4) with

$$\begin{aligned} \phi &= \phi_o + \dot{\phi} t && \text{for roll-maneuvers} \\ \theta &= \theta_o + \dot{\theta} t && \text{for pitch-maneuvers} \\ \psi &= \psi_o + \dot{\psi} t && \text{for yaw-maneuvers} \end{aligned} \qquad (4\text{-}36)$$

where ϕ_o, θ_o, ψ_o are the spacecraft roll-pitch-yaw angles at time t_o. With the quaternions determined from Equations (4-35) and (4-36), the angular velocity $\underline{\omega}$ corresponding to a given maneuver can then be obtained from Equation (4-33).

Assuming the errors in the initial and final attitudes give neglibible effect on the angular velocity computation, then the state vector for the gyro measurement can be defined as

$$\underline{X} = (G_{ij}, b_i)^T \quad (i = 1 \text{ to } 3,\ j = 1 \text{ to } 3) \qquad (4\text{-}37)$$

where G_{ij} is the component of the matrix [G] and b_i is the component of the vector $\underline{b}$.

The partial derivative equations for the gyro measurements are:

$$\frac{\partial y_i}{\partial G_{jk}} = \delta_{ij} (\omega_k + b_k) \qquad (i=1 \text{ to } 3,\ j=1 \text{ to } 3,\ k=1 \text{ to } 3)$$

$$\frac{\partial y_i}{\partial b_j} = G_{ij} \qquad (i=1 \text{ to } 3,\ j=1 \text{ to } 3)$$

4.2.7.2 Attitude Transition and Covariance Propagation

The gyro measurements can be used to calculate the state transitions and covariance propagations in a Kalman filter. The attitude transition is given by

$$\bar{q}(t_{N+1}) = \left\{ \cos\left(\frac{\omega}{2}\Delta t\right) [I] + \frac{1}{\omega} \sin\left(\frac{\omega}{2}\Delta t\right) [\Omega] \right\} \bar{q}(t_N) \qquad (4\text{-}38a)$$

$$= [M]\,\bar{q}(t_N)$$

where

$$\omega = |\underline{\omega}|$$

$$[\Omega] = \begin{bmatrix} 0 & \omega_x & -\omega_y & \omega_x \\ -\omega_z & 0 & \omega_x & \omega_y \\ \omega_y & -\omega_x & 0 & \omega_z \\ -\omega_x & -\omega_y & -\omega_z & 0 \end{bmatrix} \qquad (4\text{-}38b)$$

Assuming that all the biases considered are constant in time and coupling between attitude and biases gives negligible effects on state transition and covariance propagation, then the state transition matrix Φ, the state noise matrix Q, and the state noise transition matrix Γ are identity matrices except for the three attitude components. Let q_1, q_2, q_3 be the three independent attitude components, then the corresponding Φ, Q, and Γ are given below.

$$\phi_{ij} = \{ M_{ij} - \frac{q_j}{q_4} M_{i4} \} \quad (i,j = 1,2,3) \tag{4-39}$$

$$Q = \sigma_n^2 \quad [I] \tag{4-40}$$

where σ^2_n = the gyro noise

$= \sigma_e^2 + \sigma_\nu^2 \Delta t + \frac{1}{3}\sigma_u^2 (\Delta t)^3$

where σ_e, σ_ν, and σ_u are the standard deviations of the electronic, float torque, and torque derivative noise terms of the gyro.

$$\Gamma_{ij} = \{ [D_j] \ \bar{q} \}_i \tag{4-41}$$

where $[D_j] = \frac{1}{\omega} \sin\theta \ [\Omega_j] + \frac{\omega_j}{\omega_2} (\frac{\Delta\Delta t}{2} \cos\theta - \frac{1}{\omega}\sin\theta) \ [\Omega]$

$$\theta = \frac{\omega}{2} \Delta t$$

$[\Omega]$ is given by Equ. (4-38b)

$$[\Omega_1] = -\frac{\Delta t}{2} \omega_x [I] + \begin{bmatrix} 0 & 0 & 0 & 1 \\ 0 & 0 & 1 & 0 \\ 0 & -1 & 0 & 0 \\ -1 & 0 & 0 & 0 \end{bmatrix}$$

$$[\Omega_2] = -\frac{\Delta t}{2} \omega_y [I] + \begin{bmatrix} 0 & 0 & -1 & 0 \\ 0 & 0 & 0 & 1 \\ 1 & 0 & 0 & 0 \\ 0 & -1 & 0 & 0 \end{bmatrix}$$

$$[\Omega_3] = -\frac{\Delta t}{2} \omega_z [I] + \begin{bmatrix} 0 & 1 & 0 & 0 \\ -1 & 0 & 0 & 0 \\ 0 & 0 & 0 & 1 \\ 0 & 0 & -1 & 0 \end{bmatrix}$$

4.3 OBSERVATION ERROR AND DATA MODELING

The observation error matrix R in Eq. (3-1) and (3-2) should include the errors in the data due to both random noise and unmodeled systematic errors. However, the data errors due to unmodeled systematic errors are difficult to estimate and require a great deal of computation time to calculate from point to point. Thus, in most practices, only the estimated random error is included in the matrix R. In this case, R is defined as a diagonal matrix, with the diagonal elements equal to the square of the standard deviations of the estimated measurement errors.

In the case of observability prediction studies, the actual or simulated data is not required by GCS. The only data information required by the predictor is a scheme to specify the times at which the data is available. This scheme is referred to as "data modeling" method. For most practices, a simple data modeling method which assumes continuous data segments interleaved with specified data gaps is usually adequate to perform attitude and sensor bias observability studies.

4.4 ATTITUDE VERIFICATION

The attitude verification function compares the attitudes determined momentarily onboard with that determined from the ground using long data spans and recalibrated sensors. The standard deviation between the two types of attitudes is computed and compared with the ground attitude determination accuracy as well as the attitude accuracy requirement. If this standard deviation is higher than both the ground attitude determination accuracy and the attitude accuracy requirement, then a flag will be set

to indicate the need of updating the sensor calibration files to improve the onboard attitude determination accuracy.

The standard deviation between the onboard deterministic attitudes and the ground attitude is obtained by the following equation

$$\sigma_\theta = \left[\frac{\sum_{i=1}^{N} (\theta_i - \theta_g)^2}{N-1} \right]^{1/2} \qquad (4\text{-}42)$$

where θ_i is the i^{th} pitch, roll, or yaw angle computed onboard, θ_g is the corresponding ground attitude, and N is the total number of onboard attitudes included in the computation.

REFERENCES

1. Computer Sciences Corporation, CSC/SD-78/6082, Solar Maximum Mission (SMM) Attitude System Functional Specifications and Requirements, R.W. Byrne, P.J. Gambardella, J.A. Garber, G. Nair, D.R. Sood, and G.K. Tandon, September 1978

2. Computer Sciences Corporation, CSC/SD-79/6086, Solar Maximum Mission Attitude Determination System (SMM/ADS) User's Guide and System Description, J. Grondalski, V. Brown, H. Erickson, S. Hoven, R. Kwon, W. Lindboe, G. Nacios, and G. Neal, October 1979

3. Computer Science Corporation, CSC/SD-79/6089, Solar Maximum Mission Fine Pointing Sun Sensor (FPSS) Off-Null Calibration System (SMM/FOCS) User's Guide and System Description, J. Grondalski, J. Crowley, W. Lindboe, S. Watson, and D. Wilson, October 1979

4. Computer Sciences Corporation,CSC/TM-80/6159, Solar Maximum Mission (SMM) Attitude Analysis Postlaunch Report, G. Nair, R.H. Thompson, P.J. Gambardella, G.F. Neal, Y.R. Kwon, P.C. Kammeyer, and J.M. Buckley, August 1980

5. James R. Wertz (ed.) Spacecraft Attitude Determination and Control, Boston: D. Reidel Publishing Company, 1978

6. Computer Sciences Corporation, CSC/TR-75/6001, Multi-satellite Attitude Determination/Optical Aspect Bias Determination (MSAD/DABIAS) System Description and Operation Guide, Vol. 1, M. Joseph et.al., April 1975